Journal of Controlled Release 245 (2017) 127–136

Contents lists available at ScienceDirect

Journal of Controlled Release

journal homepage: www.elsevier.com/locate/jconrel

siRNA-cell-penetrating peptides complexes as a combinatorial therapy against chronic myeloid leukemia using BV173 cell line as model

João Miguel Freire [a,1], Inês Rego de Figueiredo [a,1], Javier Valle [b], Ana Salomé Veiga [a], David Andreu [b], Francisco J. Enguita [a,*], Miguel A.R.B. Castanho [a,*]

[a] Instituto de Medicina Molecular, Faculdade de Medicina, Universidade de Lisboa, Av. Prof. Egas Moniz, 1649-028 Lisbon, Portugal
[b] Department of Experimental and Health Sciences, Pompeu Fabra University, Barcelona Biomedical Research Park, E-08003 Barcelona, Spain

ARTICLE INFO

Article history:
Received 26 April 2016
Received in revised form 21 November 2016
Accepted 23 November 2016
Available online 24 November 2016

Keywords:
Chronic myeloid leukemia
Bcr-Abl
siRNA
Dengue virus capsid protein
Cell-penetrating peptide
Bioportide
Microarray

ABSTRACT

Chronic myeloid leukemia (CML) is a myeloproliferative disorder caused by a single gene mutation, a reciprocal translocation that originates the Bcr-Abl gene with constitutive tyrosine kinase activity. As a monogenic disease, it is an optimum target for RNA silencing therapy. We developed a siRNA-based therapeutic approach in which the siRNA is delivered by pepM or pepR, two cell-penetrating peptides (CPPs) derived from the dengue virus capsid protein. These peptides have a dual role: siRNA delivery into cells and direct action as bioportides, i.e. intracellularly bioactive CPPs, targetting cancer-related signaling processes.

Both pepM and pepR penetrate the positive Bcr-Abl^{+} Cell Line (BV173). Five *in silico* designed anti-Bcr-Abl siRNA were selected for *in vitro* analysis after thorough screening. The Bcr-Abl downregulation kinetics (48 h to 168 h) was followed by quantitative PCR. The bioportide action of the peptide vectors was evaluated by genome-wide microarray analysis and further validated by testing BV173 cell cycle and cell proliferation monitoring different genes involved in housekeeping/cell stress (RPL13A, HPRT1), cell proliferation (ki67), cell apoptosis (Caspase 3 and Caspase 9) and cell cycle steps (CDK2, CCDN2, CDKN1A). Assays with a commercial transfection agent were carried out for comparison purposes. Maximal Bcr-Abl gene knockdown was observed for one of the siRNA when delivered by pepM at 120 h. Both pepM and pepR showed downregulation effects on proliferative CML-related signaling pathways having direct impact on BV173 cell cycle and proliferation, thus reinforcing the siRNA effect by acting as anticancer molecules.

With this work we show the therapeutic potential of a CPP shuttle that combines intrinsic anticancer properties with the ability to deliver functional siRNA into CML cell models. By such combination, the pepM-siRNA conjugates lowered Bcr-Abl gene expression levels more extensively than conventional siRNA delivery technologies and perturbed leukemogenic cell homeostasis, hence revealing their potential as novel alternative scaffolds for CML therapy.

© 2016 Elsevier B.V. All rights reserved.

1. Introduction

Chronic myeloid leukemia (CML) is a myeloproliferative disorder originated from a neoplastic transformation in blood pluripotent stem cells, progressing from a chronic to an acute phase [1–3]. This malignancy is commonly associated to the chromosomal rearrangements involving the Abelson murine leukemia viral oncogene homolog 1 (*ABL1*) and the breakpoint cluster region (*BCR*), which leads to gene truncation and appearance of the unregulated and constitutively expressed *Bcr-Abl* fusion gene in the Philadelphia (Ph) chromosome [1–3] (Fig. 1).

The loss of *ABL1* regulation in the *Bcr-Abl1* fusion oncoprotein results in active tyrosine kinase (TK) activity [3,4] leading to uncontrolled signaling that modulates differentiation, proliferation, migration, adhesion and decreased apoptosis processes [3] that constitute the hallmark of CML.

At present, CML therapy relies on finely tuned TK inhibitors (TKIs) [3,5] such as first-in-class imatinib (Gleevec®) [3,5]. TKIs compete with ATP for the ABL binding site, stabilizing the inactive kinase-domain conformation and preventing it to switch to the active state [6]. Despite its considerable clinical success, TKI monotherapy is not curative and prolonged treatment is known to induce resistance and tolerance (due to *Bcr-Abl1* gene point mutations), which has prompted the introduction of next-generation TKIs [5,7]. In such a context, the development of novel and safer therapies alternative to 2nd and 3rd generation TKIs [3] is not only sensible but highly desirable as a long-term strategy.

* Corresponding authors.
E-mail addresses: fenguita@medicina.ulisboa.pt (F.J. Enguita), macastanho@medicina.ulisboa.pt (M.A.R.B. Castanho).
[1] The authors contributed equally to this work.

http://dx.doi.org/10.1016/j.jconrel.2016.11.027
0168-3659/© 2016 Elsevier B.V. All rights reserved.

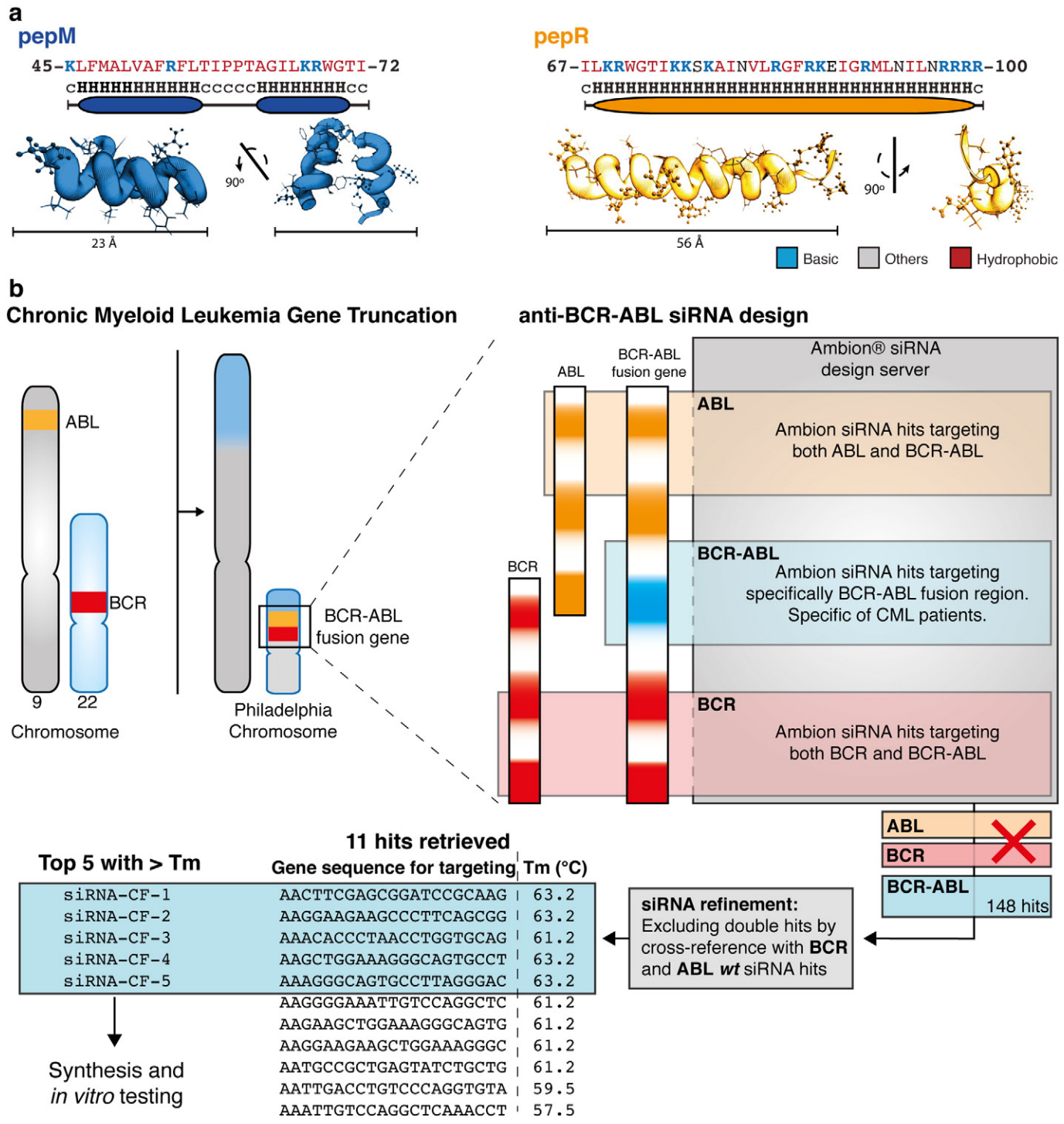

Fig. 1. Design of the CML siRNA therapy targeting Bcr-Abl1 gene. **a)** Sequence and tridimensional representation of two viral CPPs derived from Dengue virus capsid protein, pepM (blue) and pepR (orange). Positively charged residues (blue), hydrophobic and non-charged residues (red) and negatively charged residues (black) are shown (adapted from Freire et al. [27]). **b)** Schematic representation of chromosome 9 and 22 highlighting the *ABL1* (orange) and *BCR* (red) and the chromosomal rearrangement originating the Philadelphia chromosome with the *Bcr-Abl1* (p190 mutation). Workflow of the prediction and design of the *Bcr-Abl1* mRNA regions to be targeted with siRNA and filtering process using the *wt BCR* and *ABL* sequence hits. Final selection of the top 5 mRNA sequence regions was done according to the highest melting temperature (Tm).

The use of short-interfering/short-hairpin RNA (siRNA/shRNA) technology to down-regulate *Bcr-Abl1* gene has been reported to fight CML [8–10]. Gene therapy is an ideal approach for monogenic diseases such as CML, caused by the single *Bcr-Abl1* mutation. Knowing the target gene sequence, it is possible to design a siRNA that, when delivered into the cell will selectively interact with the mRNA and hamper protein expression. To this end, in addition to the specific siRNA, a functional, effective and non-toxic vector for siRNA cellular delivery is required. Finding such a vector is the main limitation of this, otherwise promising, therapeutic approach [11] as the plasma membrane constitutes an effective barrier for most hydrophilic molecules [11–13]. Being negatively charged, siRNAs do not easily penetrate hydrophobic cellular membranes and, if unprotected and unmodified, are generally rapidly degraded in the serum. Physical/mechanical processes and viral vectors

are widely used, however they induce high cellular damage/death and safety risks due to immune responses and inflammation, respectively. Non-viral technologies (liposomes, nanoparticles or cell-penetrating peptides – CPPs) are a better option for gene delivery due to lower toxicity levels and absence of immune response [11]. CPPs have the ability to translocate across biological membranes in a non-disruptive way [11–13], and would therefore be ideal vectors to deliver *Bcr-Abl1* siRNA, as amply demonstrated for a plethora of drugs used to treat multiple disorders [14–16]. CPPs are typically 9-35mer cationic (Lys and/or Arg-rich) and/or amphipathic peptides [12,17–19], widely studied over the last 20 years as delivery vectors for biological payloads such as small RNA/DNA, plasmids, antibodies and nanoparticles [20,21]. Their biomedical application for gene therapies [11], by delivering siRNA, genes and plasmids [12,20–23], has been well established in recent years. Moreover, while carrying cargos into the cell, some CPPs may act as bioportides, i.e. have an effect on cell metabolism, by interfering with the cell cycle or apoptotic routes [24,25].

We are interested in designing CPP-siRNA complexes in which the delivery vector will act as a bioportide, to increase the therapeutic effect of the formulation (perturbing proliferation signaling pathways and cell cycle checkpoints, among others). In this work we evaluate the ability of pepR and pepM, two CPPs derived from dengue virus capsid protein (DENV C) recently developed in our labs [26,27], to deliver anti-*Bcr-Abl1* siRNA into CML cells and act as antitumor bioportides against CML. This innovative approach may entail a strong improvement in the efficacy of the treatment, reducing the dosage needed and long-term acquired resistance. These peptides and the full DENV C proteins were used recently to successful deliver anti-DENV siRNA molecules in order to inhibit DENV infection, as well as anticancer siRNAs targeting cell proliferation [28]. In this work, $Ph1^+$ human cell line BV173 [29] was used as a CML cell model. Similar studies have been performed by others using a leukemia cell line as the model of the disease [9,10,30]. The specific usage of BV173 is explained by the *Bcr-Abl1* mutation present in the cell line (p190 mutation). *Bcr-Abl1* fusion gene translation may result in different proteins [1] due to alterative splicing, thus a significative aspect to take into consideration when designing the siRNA molecules. The 5 novel siRNA molecules targeting the *Bcr-Abl1* mRNA were designed accordingly to BV173 mutation. The molecules were then delivered by means of either pepM or pepR mediated transport. Moreover, the influence of pepR and pepM on the regulation of *Bcr-Abl1* expression was investigated in a genome-wide study on the effect of both CPPs in BV173 expression patterns, while cell proliferation, homeostasis and apoptosis was evaluated by microarray and cell cycle analysis. To corroborate the microarray data, quantitative PCR (qRT-PCR) was performed to different genes involved in housekeeping/cell stress (RPL13A, HPRT1), cell proliferation (ki67), cell apoptosis (Caspase 3 and Caspase 9) and cell cycle steps (CDK2, CCDN2, CDKN1A).

CML is a complex, high incidence disease that constitutes a huge social burden. The limitations in the currently available treatments call for new approaches to fight this disease, such as CPP-mediated siRNA and/or gene editing, whereby simultaneous CPP delivery and bioportide effects could play a crucial enabling role.

2. Materials and methods

2.1. Chemicals

Fmoc-protected amino acids, Fmoc-Rink-amide (MBHA), 2-(1H-benzotriazol-1-yl)-1,1,3,3-tetramethyluronium hexafluorophosphate (HBTU) and N-hydroxybenzotriazole (HOBt) were from Iris Biotech (Marktredwitz, Germany). HPLC-grade acetonitrile, and peptide synthesis-grade N,N-dimethylformamide (DMF), dichloromethane (DCM), N,N-diisopropylethylamine (DIEA) and trifluoroacetic acid (TFA) were from Carlo Erba-SDS (Sabadell, Spain). Minimum essential medium α (α-MEM), Dulbecco's modified Eagle's medium (DMEM), fetal bovine serum (FBS), penicillin-streptomycin (Pen-Strep), phosphate buffer saline (PBS), the fluorescent dyes Hoechst 33342, were purchased from Life Technologies (Carlsbad, CA, USA). All other reagents were of the highest quality available commercially. All experiments were performed using 10 mM HEPES buffer, pH 7.4, in NaCl 150 mM, unless otherwise stated.

2.2. siRNA design

The specific usage of BV173 is explained by the *Bcr-Abl1* mutation present in the cell line. *Bcr-Abl1* fusion gene translation may result in different proteins [1] due to alterative splicing, thus a significative aspect to take into consideration when designing the siRNA molecules. The 5 novel siRNA molecules targeting the *Bcr-Abl1* mRNA were designed accordingly to BV173 mutation. siRNA to target specifically the boundary regions of the fusion *Bcr-Abl1* gene were predicted with the siRNA Target Finder from Ambion® (Life Technologies, Carlsbad, CA, USA). The *Bcr-Abl1* mRNA sequence (gi:162135197) was submitted to the server retrieving 147 gene sequence targets (Supplementary section 1, Table 1). To refine the siRNA hits both *wt BCR* and *ABL* genes (gi:29411 and gi:177942, respectively) were submitted to Ambion® server and the hits were cross-referenced and filtered with the previously 147 *Bcr-Abl1* gene targets. Only the siRNA for sequences that were specific for *Bcr-Abl1* were considered (11 mRNA sequences – Supplementary Section 1, Table 2). The top 5 siRNA pairs (5′-siRNA-3′ and 3′-siRNA-5′ for each mRNA sequence) were selected considering the highest melting temperature (Tm °C), which reflects better nucleotide hybridization, thus better mRNA expression inhibition. The siRNA-CF-1 (5′-CUUCGAGCGGAUCCGCAAGtt-3′, 3′-CUUGCGGAUCCGCUCGAAGtt-5′), siRNA-CF-2 (5′-GGAAGAAGCCCUUCAGCGGtt-3′, 3′-CCGCUGAAGGGCUUCUUCCtt-5′), siRNA-CF-3 (5′-ACACCCUAACCUGGUGCAGtt-3′, 3′-CUGCACCAGGUUAGGGUGUtt-5′), siRNA-CF-4 (5′-GCUGGAAAGGGCAGUGCCUtt-3′, 3′-AGGCACUGCCCUUUCCAGCtt-5′) and siRNA-CF-5 (5′-AGGGCAGUGCCUUAGGGACtt-3′, 3′-GUCCCUAAGGCACUGCCCUtt-5′) that, respectively, target *Bcr-Abl1* gene regions of 5-AACTTCGAGCGGATCCGCAAG-3, 5-AAGGAAGAAGCCCTTCAGCGG-3, 5-AAACACCCTAACCTGGTGCAG-3, 5-AAGCTGGAAAGGGCAGTGCCT-3, 5-AAAGGGCAGTGCCTTAGGGAC-3 were purchased from Ambion® for *in vitro* testing against *Bcr-Abl1* in the CML cell model.

2.3. pepR and pepM

Both pepR (LKRWGTIKKSKAINVLRGFRKEIGRMLNILNRRRR –residues 67–100 of DENV-2C protein) and pepM (KLFMALVAFLRFLTI PPTAGILKRWGTI – residues 45–72 of DENV-2C protein), were assembled by solid phase synthesis on Fmoc-Rink-amide MBHA resin in a Prelude peptide synthesizer (Protein Technologies, Tucson, AZ) running standard Fmoc chemistry protocols [31] at 0.1 mmol scale, as described earlier [32–34]. Details on synthesis and purification are given in [26,27]). The HPLC-purified peptides were satisfactorily characterized by MALDI-TOF MS. pepR and pepM tridimensional structures were predicted at I-TASSER web-server [35] (http://zhanglab.ccmb.med.umich.edu/I-TASSER/I-Tasser). The molecular representation of the peptides were done in Pymol v1.4 [36].

2.4. Cell culture

$Ph1^+$ human cell line BV173 [29] were cultured in RPMI-1640 medium supplemented with 10% FBS and 100 U mL^{-1} of penicillin/streptomycin, at 37 °C in a humidified atmosphere of 5% CO_2. Cells were counted using a Fuchs-Rosenthal hemocytometer (Brand Wertheim, Wertheim, Germany) and their viability was determined by the trypan blue dye exclusion method.

2.5. Confocal microscopy

BV173 cell suspension of 2×10^4 cells mL^{-1} were added in 24-well plates and cultured for 2 days. An inverted confocal point-scanning Zeiss LSM 510 META microscope equipped with Diode 405-30, Argon2, DPSS 561-10, HeNe 594 and HeNe 633 lasers, and a temperature control incubator (37 °C) with CO_2 supply was used. Images were taken on with a Plan-Aprochromat 63× objective (Zeiss, Jena, Germany). Nucleus was stained with DAPI (1 mg mL^{-1}). All images were analyzed by the image processor Fiji [37].

2.6. pepR- and pepM-mediated pGFP transfection into BV173.

pEGFP transfection experiment was performed according to previous studies [26,27]. BV173 cells were seeded onto a 24-well plate (2×10^5 cells mL^{-1} in each well) and cultured for 24 h. Then, 1 μg of the pEGFP-C3 plasmid pre-incubated with either 2 μM of pepR or pepM, or FuGENE®, was added to the cultures. After 6 h, the culture medium was replaced by fresh medium. 48 h post-transfection, cells were harvested, washed 3 times with PBS and positive transfection was followed by cell fluorescent emission due to the expression of GFP by confocal microscopy. Quantitative image analysis was computed in order to count the percentage of transfected cells, identified by the nuclear staining dye DAPI and to evaluate the transfection efficacy on each cell measuring the average fluorescence intensity of each transfected cell (Supplementary section 2 for more details).

2.7. Bcr-Abl1 gene silencing by custom siRNA

Bcr-Abl1 gene silencing assay was performed at BV173 cell culture. After 24 h of culture, BV173 were transiently transfected for silencing of *Bcr-Abl1* gene using small interfering RNA (siRNA-CF-1 to siRNA-CF-5, previously mentioned). Transfection was performed with 16 nM of each sense and anti-sense siRNA pair using Fugene® or pepR and pepM (at peptide:siRNA molar ratio of 5:1) for 6 h, according to the manufacturer's instructions. Previous studies in the lab had already provided deep biophysical and molecular characterization on either pepR or pepM peptide:nucleic acids complexes formed, their interaction with lipid membranes and their putative cellular entry mechanism [26,27]. Moreover peptide-nucleic acids binding constants, complex size and stoichiometry (4:1 for pepR and 2.5:1 for pepM) has also been carefully assessed previously by FRET and DLS experiments [33,34], as such we dedicated the article on exploring these formulations and molecules as anticancer approaches for CML. For the screen of the 5 siRNA molecules, the silencing of *Bcr-Abl1* gene was analyzed by real-time PCR 72 h after transfection. For the screen of the best 2 siRNA candidates and the evaluation of pepR and pepM effective transfection, quantitative PCR (qRT-PCR) was performed 96 h post-transfection. The kinetic study of siRNA-CF-3 was followed by qRT-PCR 48 h, 72 h, 96 h, 120 h and 168 h after siRNA transfection. Cells were harvested and lysed with TRIZOL reagent (Life Technologies,Carlsbad, CA, USA). Total RNA was treated with DNAse I (Fermentas, Burlington, Ontario) and first strand cDNA was synthesized using 2 μg of the extracted RNA using High-Capacity cDNA Archive Kit (Life Technologies) according to the manufacturer's instructions. cDNA was diluted 1:5 and 1 μL of each sample was used for qRT-PCR using Power SYBR Green PCR master mix (Life Technologies). *Bcr-Abl1* gene fusion identification and quantification was performed using the primers Forward 5′ – CAGATGCTG ACCAACTCGTGT – 3′, and Reverse 5′ – TTCCCCATTGTGATTATAGCCTA – 3′ [38]. GAPDH (Glyceraldehyde 3-phosphate dehydrogenase) gene was used as housekeeping normalizer. The differences between the relative expression values for the *BCR-Abl1* gene in the control (only pepR and pepM) and siRNA transfected samples were submitted to a two-tailed *t*-test to ascertain their statistical significance. The resulting data are the mean of three experiments with standard deviation.

2.8. pepR and pepM effects in gene expression of BV173 (Microarray)

For mRNA analysis total RNA was extracted from cell cultures using Trizol (Life Technologies) and further purified with the Qiagen RNAeasy kit. RNA quality and quantity was assessed using the Bioanalyzer RNA nano-chip (Agilent Technologies, Waldbronn, Germany) and NanoDrop (Thermo Scientific, Waltham, MA, USA), respectively. Each sample (5 μg) was reverse transcribed by SuperScript III RNAse-H reverse transcriptase (Life Technologies) using random primers. The cDNAs were hybridized to Affymetrix human HuGene-2.0-ST microarrays (Affymetrix, Inc., Santa Clara, CA, USA) following the protocol described by the manufacturer in the Genecore EMBL facility (Heidelberg, Germany). Data were deposited in NCBI Gene Expression Omnibus. Microarray raw data was processed with the Affymetrix transcriptome analysis console software. Briefly, raw CEL data files from the scanned arrays were normalized by the RMA algorithm. Probesets with DABG (detection above background) *p*-values above 0.5 or non-log expression below 1.0 were previously removed from the analysis. A moderate *t*-test analysis was used for pairwise comparisons between sample groups. Only genes with raw *p*-values < 0.05 and fold-change > 2 were considered as differentially expressed.

Validation of the expression of selected mRNA transcripts involved in apoptosis (CASP3 and CASP9), cell cycle (CDK2, KI67, CCNA2 and CDKN1A) and house-keeping (RPL13A and HPRT1) was performed by qRT-PCR using the primers in the Supplementary Table S3 in Section 4.

2.9. BV173 cell cycle

BV173 cell cycle analysis was performed by flow cytometry analysis using Hoechst 33342 DNA staining dye as described [39,40]. Flow cytometry experiments were performed using a BD LSR Fortessa from BD Biosciences (San Jose, CA, USA) equipped with 3 lasers (violet – 405 nm, blue – 488 and red – 640 nm). Briefly, BV173 were cultured and pepR or pepM were added to the cell suspension at 0.5 or 5 μM. 48 h after each peptide incubation, cells were stained with Hoescht 33342 (1 μg mL^{-1}) and measured in the cytometer. The linear scale histograms were analyzed with Watson pragmatic model for cell cycle [41] in order to deconvolute the cell population into G0/G1, S and M/G2 populations.

3. Results and discussion

In this work we evaluated the ability of pepR and pepM, two DENV C protein-derived CPPs, to deliver anti-*Bcr-Abl1* siRNA to CML cells with a combinatorial therapeutic action: a direct effect of siRNA on *Bcr-Abl1* expression levels with concomitant decreasing of cell-signaling proliferation, plus CPP-induced perturbation of cell cycle checkpoints. To this end, we designed new siRNAs with specific *Bcr-Abl1* targeting, selected the best candidate and evaluated the therapeutic effect of the CPP-siRNA conjugate on a CML cell model.

3.1. siRNA design and GFP cell transfection to BV173

The methodology used to design siRNAs targeted to the *Bcr-Abl1* fusion region retrieved 147 potential sequences (Supplementary information Section 1 – Table S1). The list was further refined using a comparative approach with the *wt* BCR and ABL sequences (Fig. 1), which yielded 11 potential *Bcr-Abl1* specific sequences from which those 5 with the highest estimated melting temperature were selected (Supplementary information Section 1 – Table S2), as illustrated in Fig. 1. $Ph1^+$ human cell line BV173 [29] was used as a CML model. The ability of pepR and pepM to enter BV173 cells was evaluated by transfecting a GFP-encoding plasmid with either these CPPs or a commercial transfection agent (FuGENE®) and comparing the results by GFP imaging by confocal microscopy (Fig. 2a, b). Both CPPs were shown to be more efficient than the standard application (Fig. 2b), providing higher

number of transfected cells and higher average GFP fluorescence intensity per cell, suggesting more plasmid copies delivered and/or better plasmid release promoting functional GFP translation (Supplementary Section 2 – Fig. S1). Hence pepM and pepR can efficiently transfect genomic material into the CML cell model.

3.2. siRNA screening for Bcr-Abl1 silencing

As mentioned above, 5 siRNA molecules targeting the *Bcr-Abl1* mRNA were selected (Fig. 1 and Table S2) for *in vitro* testing when delivered with either pepM or pepR. A 3-stage screening was applied: first a commercial transfection agent was used to test the anti- *Bcr-Abl1* mRNA. Using an established transfection agent would discard lack of downregulation due to ineffective delivery by our CPP molecules. Moreover, one could select from the siRNA pool which of the 5 siRNA molecules was more effective (Fig. 2c). In a following step the most successful and promising siRNA, together with a non-effective siRNA (Fig. 2a), was delivered to cells by either pepR or pepM and the siRNA efficacy was again evaluated (Fig. 2b). The selection of a non-effective siRNA allow us to have significant and comparable downregulation data in what respects to the CPP delivery efficiency and siRNA effect.

Finally, the kinetics of the best candidate to down-regulate *Bcr-Abl1* (siRNA-CF-3) was studied, in order to evaluate the time-span of action of these molecules *in vitro* and prospect about its putative pharmacokinetics *in vivo* (Fig. 3c). When compared to the commercial transfection agent, which is active for 96 h with modest results, pepM-mediated siRNA delivery achieved longer (120*h*) effect on *Bcr-Abl1* downregulation. In particular, pepM-siRNA-CF-3 was shown to be a powerful candidate for further development as CML therapy. This result is consistent with published data on siRNA action: recruitment and assembly of the RISC/mRNA complex and Argonaute system action to inhibit gene expression has a 2–5-day time-span after transfection, depending on the siRNA concentration and transfection agent efficiency [42]. In order to evaluate off-target and unspecific target by the siRNA that would interfere with cell homeostasis and proliferation qRT-PCR of housekeeping/cell stress (RPL13A, HPRT1), cell proliferation (ki67) and apoptosis genes (Caspase 3 and Caspase 9) was assayed.

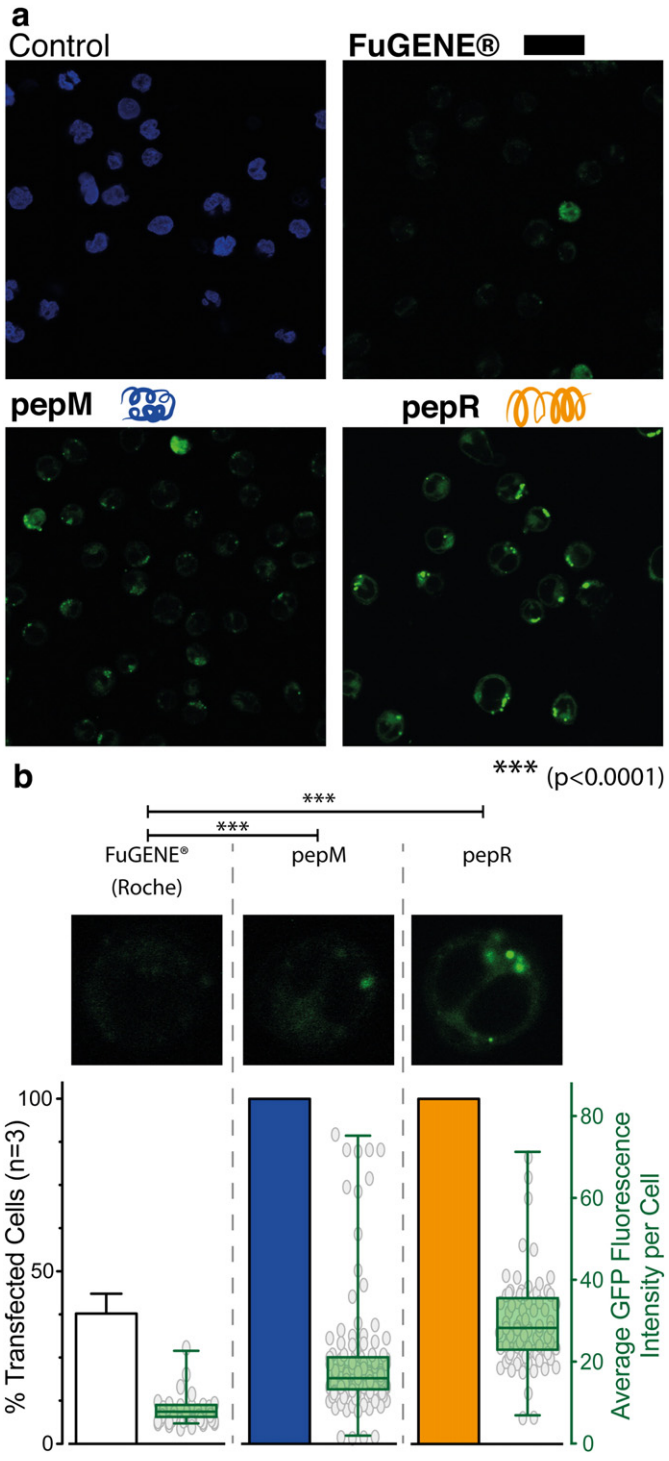

Fig. 2. Quantification of BV173 GFP transfection mediated by Fugene®, pepM and pepR. **a)** Confocal imaging of BV173 cells cultured for one day and then transfected with GFP-encoded plasmid using FuGENE®, pepM or pepR (control – no transfecting agent). Positive GFP expression (green) was imaged 48 h after transfection. Nuclear staining with DAPI – blue. **b)** *top panel* - Confocal image of a representative GFP transfected BV173 cell with GFP-encoded plasmid using FuGENE®, pepM or pepR showing GFP protein fluorescence emission (green). Percentage of transfected cells over the total number of cells was determined (white bars – mean ± SD) as well as the average GFP (green) fluorescence intensity of the transfected cells (green box – *mean* ± *SD*, and whiskers – min to max). Each measured cell is represented as grey circles at the background of the box and whisker plot. Average fluorescence intensity values between transfection agents were analyzed by a two-tailed *t*-test (*** - $p < 0.0001$, $n > 3$).

3.3. Gene regulation of leukemia cells by pepR and pepM

The main purpose of the gene expression analysis was to characterize the gene expression profile induced by the peptides alone. As already described in the literature, peptide-based molecules may induce cell stress and immunological responses [11,13,15]. Moreover, Kuo et al. [43] pinpointed the genome-wide effects of octoargine (R8), a synthetic CPP [17], in U-937 human macrophages mapping the production of cytokines induced by R8 (TNF-α, IL-1β and IL-6). Thus, we intended to, while observing the potential cell stress caused by the presence or pepR or pepM, to obtain specific data that directly correlates to the anticancer application of these peptides. Moreover, to highlight their potential molecular targets to explain such antitumor action. Regarding gene expression profiles of siRNA action in CML cells, some studies performed by Ohba *et al.* [64] and Huang *et al.* [65] have already reported such alterations, an additional reason to not follow such study as is would not retrieve no additional knowledge, and would hide the peptide-specific-induced alterations. Performing siRNA-CPP microarray would not allow us to isolate specific alterations induced by the peptides as they could be assigned to the siRNA effect on downregulating BCR-ABL and the overall cell consequences on that reduction.

The influence of isolated pepR and pepM on *Bcr-Abl1* expression regulation was also evaluated (Supplementary Section 3). A genome-wide study on the effect of both CPP in BV173 expression patterns revealed that most genes differentially expressed in response to pepR and pepM are miRNAs (9% and 31% of the differentially expressed genes, respectively – Fig. 4b). Genes with significant altered expression levels

relative to control cells [44] were analyzed (Fig. 4c and Supplementary Table 3). Specifically, each identified down- or up-regulated miRNA (Fig. 4c) was analyzed in order to predict its putative mRNA targets and consequent influence on BV173 cell proliferation and homeostasis. miRNAs are small non-coding RNAs that negatively regulate specific mRNA at the post-transcriptional level, also acting as all-in-one pathway regulators [45–48]. Using the miRBase [49] database, which integrates a plethora of miRNA analysis tools such as TARGETSCAN v6.2 [50], DIANA-microT v5.0 [51] and DIANA-miRPath [52], we estimated the pathways that pepM or pepR, by means of miRNA alterations, were influencing during siRNA delivery (Supplementary Table S4.xls). Fig. 4d condenses the cancer-related pathways that are significantly altered due to miRNA level changes caused by pepR or pepM (miR-4729, miR-133a, miR-548n, and miR-1323). Most of the pathways identified are major signaling pathways involved in the regulation of several proliferative processes, commonly associated to oncogenesis (p53, Wnt, PI3K-Akt and MAPK signaling pathways), as well as cell cycle [53–55]. Moreover, cellular/membrane traffic routes involved in the dynamics of cytoskeleton and endocytic vesicles were up-regulated. This is not surprising given the mode-of-action of those CPPs when delivering nucleic acids [27]. Cytoskeleton rearrangements have already been reported upon internalization of Tat-cargo conjugates [56] but CPPs had never been identified as responsible for promoting the increase on cytoskeleton gene expression by themselves. To address and consolidate this observation we quantified the actin mRNA expression levels during siRNA delivery by pepR and pepM (Fig. 4b). We evaluated the influence of pepR and pepM inducing actin mRNA expression by comparing the delivery of equimolar amount of the peptides alone, against the siRNA:peptide complexes, which would indicate if actin mRNA levels are a consequence of siRNA presence and siRNA machinery or strictly to pepR or pepM delivery mechanism of action. Fig. 4b clearly shows that the addition of only either pepR or pepM caused nearly 3-fold increase in actin's mRNA expression levels.

In order to investigate the influence that either pepR or pepM have on cancer-related proliferative pathways and BV173 cell cycle directly (heatmaps from Fig. 4d), we performed cell cycle analysis using the Hoechst 33342 nuclear staining dye [39,40] (Fig. 5), which allows to evaluate the effect of these vectors on cell division and homeostasis. Two limit concentrations were used: 0.5 μM, the minimal amount of vector required to successfully deliver siRNA and GFP plasmids, and 5 μM, a 10-fold higher concentration intended to assess the influence of these peptides on BV173 cell homeostasis at an extreme stress, while still below cytotoxic levels [26]. Regardless of the concentration, a significant decrease on the percentage of cell population in the M/G2 phase was observed for both peptides. Consistently, the proliferative signaling pathways identified in Fig. 4C heatmaps are checkpoints at G2/M cell cycle stages (p53, MAPK, Wnt) [57–59]. To validate such correlations, several cell cycle checkpoint genes (CDK2, CCDN2, CDKN1A) were monitored throughout the kinetics of siRNA delivery by pepM and FuGENE by qRT-PCR. Moreover, we also monitored proliferation (ki67 [60]) and apoptosis genes (Caspase 3 and Caspase 9) during this period. The overall results are depicted in Fig. 6. The combination of the genes monitored by qRT-PCR highlights the antitumor activity of pepM while delivering the siRNA molecules rather than performing solely as a delivery agent, as FuGENE. One can observe that neither FuGENE or pepM induce apoptosis (Fig. 6a and d, respectively) or major alterations on basal cell protein expression (Figs. 6c and f, respectively) by following RPL13A (60S ribosomal protein L13a) and HPRT1 (Hypoxanthine Phosphoribosyltransferase 1) as housekeeping genes. As for the cell cycle genes analysis (Fig. 6b and e for FuGENE and

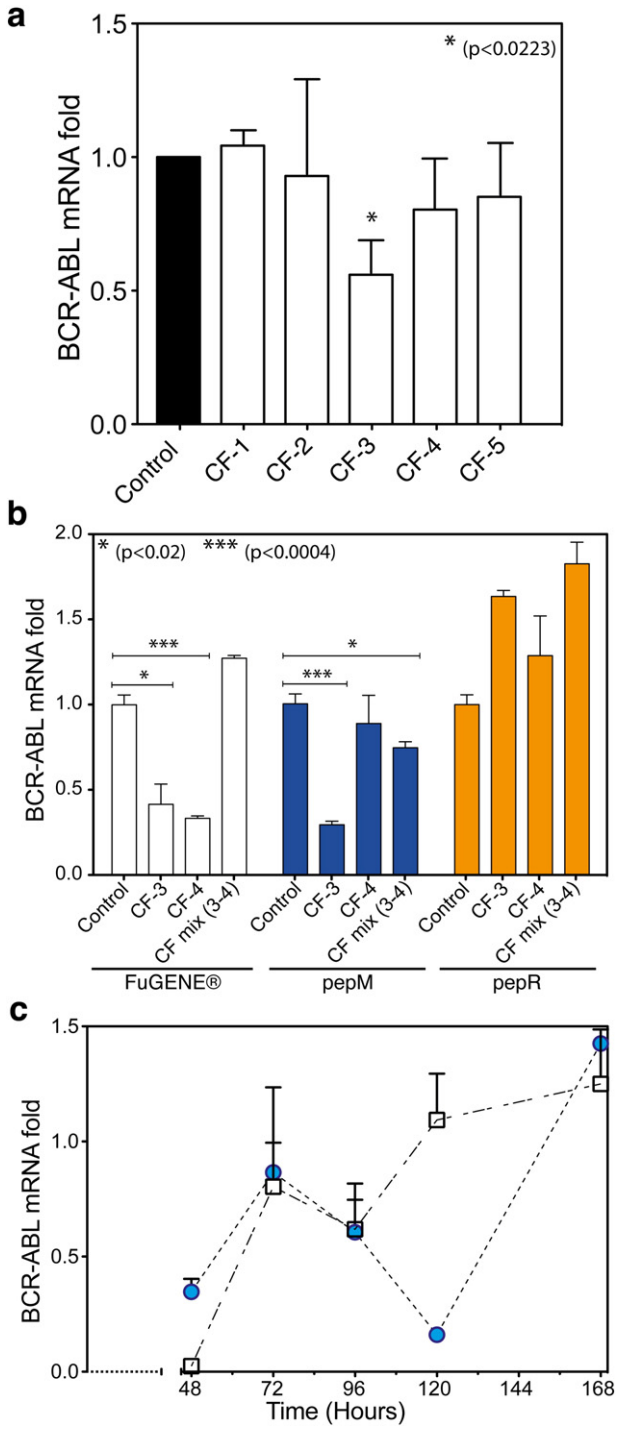

Fig. 3. Quantification of siRNA-mediated *Bcr-Abl1* downregulation in BV173 cells. **a)** *Bcr-Abl1* gene silencing assays using the synthesized siRNA-CF-1 to siRNA-CF-5. Transfection was performed using FuGENE® (white) to screen for the most effective siRNA to be further delivered by pepM or pepR. mRNA expression levels were analyzed by real-time PCR 72 h after transfection. Results reflect *Bcr-Abl1* expression changes in the presence and absence (black) of each siRNA-CF-# (# ranges from 1 to 5). Relative expression values were analyzed by the two-tailed *t*-test (*** - $p < 0.0001$; * - $p < 0.0223$). **b)** *Bcr-Abl1* gene silencing assays using the most promising siRNA candidates from Fig. 3a: siRNA-CF-3 and siRNA-CF-4. Transfection was performed using FuGENE® (white), pepM (blue) or pepR (orange). mRNA expression levels were analyzed by real-time PCR 96 h after transfection. Results reflect *Bcr-Abl1* expression changes in the presence and absence of each siRNA-CF-# (# ranges from 3 to 4) for each transfection agent tested. Relative expression values were analyzed by the two-tailed *t*-test (*** - $p < 0.0004$; * - $p < 0.02$). **b)** Kinetic of *Bcr-Abl1* gene silencing assay using the optimal siRNA designed (Fig. 3b) siRNA-CF-3. Transfection was performed using FuGENE® (white squares) and the viral CPP vector that showed to be the best candidate, pepM (blue circles). mRNA expression levels were analyzed by real-time PCR 48 h, 72 h, 96 h, 120 h and 168 h after transfection. In every case, the resulting data are the mean of three experiments with standard deviation.

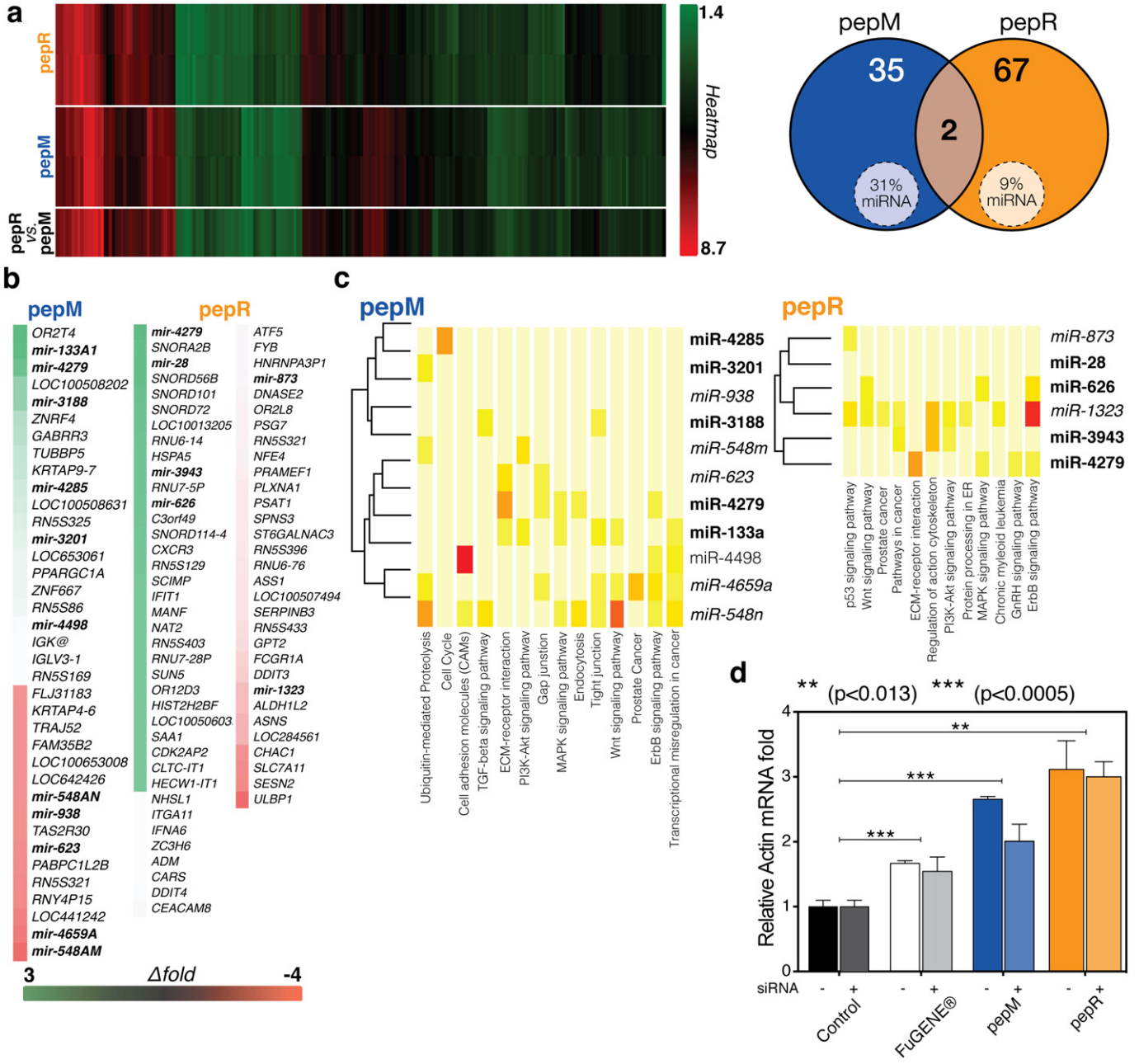

Fig. 4. Gene expression changes in BV173 cells induced by pepR or pepM. **a)** Genome-wide expression pattern of BV173 cells in the presence of either pepM or pepR (0.2 μM). Heatmap representation shows a clustered display of data from BV173 cells incubation with pepR and pepM (the dendrogram and colored expression map image were produced in Affymetrix transcriptome analysis console software; the color scale ranges from saturated green (1.4) to saturated red (8.7). Data were measured using a Affymetrix human HuGene-2.0-ST microarrays (Affymetrix, Inc., Santa Clara, CA, USA) and are deposited in NCBI Gene Expression Omnibus (awaiting approval). All measurements are relative to BV173 cells alone. Genes were identified for analysis as down- or up-regulated if the expression level deviated from control cells by a factor of 1.5. The selected regulated genes for pepM or pepR were plotted in a Venn diagram (*right panel*). **b)** List of over- and under-expressed genes in BV173 cells after incubation with pepR or pepM. The color scale ranges from saturated green for fold variation log ratios of 3.0 and below to saturated red for fold variation log of −4. Each gene is represented by a single row of colored boxes. **c)** Analysis of cellular pathways that are modulated by miRNA that were up-regulated (**bold**) or down-regulated (*italic*) after incubation with pepM or pepR. The miRNA DIANA server package with the miRPath v2.0 [58] and microT v5.0[59] online tools were used to predict and evaluate the pathways being modulated and perturbed by the target miRNA. The color scale ranges from high significant pathway prediction *p*-value score (−15 – *red/orange* – in log scale) to lower prediction confidence levels with *p*-value score of 0 (*light yellow*). **d)** Actin expression levels in BV173 cells after delivery of siRNA-CF-3. mRNA expression levels were analyzed by quantitative real-time PCR 96 h after transfection. Results reflect Actin expression changes in the presence and absence of siRNA-CF-3 for each transfection agent tested (FuGENE® or 0.2 μM of pepR or pepM). Relative expression values were analyzed by a two-tailed *t*-test (*** - $p < 0.0005$; ** - $p < 0.013$). The resulting data are the mean of three independent experiments with standard deviation.

pepM, respectively), the data corroborates with the kinetics of siRNA delivery depicted in Fig. 4c. By interpreting the ki67 and CDK2, CCDN2, CDKN1A expression levels of pepM, these reach their minimum around 120 h, time where we encounter the second minimum of the BCR-ABL mRNA expression. Comparing with the commercial agent, not having an anticancer action *per se* and acting solely as a drug delivery agent, this profile does not occur and thus no prolonged anti-CML is observed.

It is worth highlighting however that there is no complete cell cycle arrest. The siRNA is needed in conjugation with the peptides for an

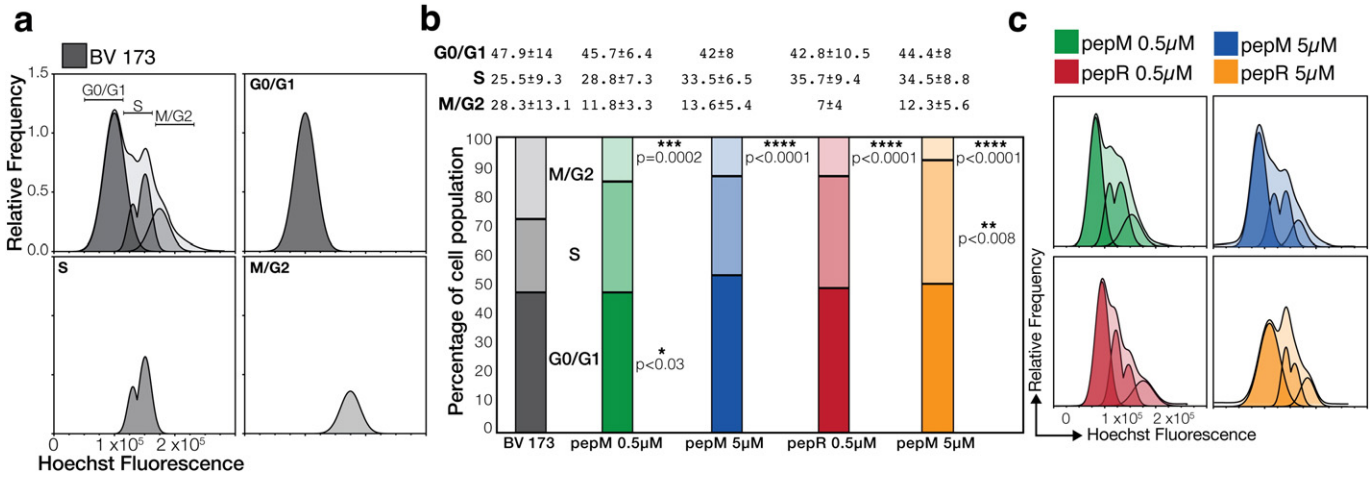

Fig. 5. pepR and pepM influence on BV173 cell cycle. BV173 cell cycle analysis intended to evaluate the overall influence of either pepR or pepM on the proliferative kinase pathways identified indirect targets in the microarray analysis. Hoechst 33342 DNA fluorescent staining dye was used to follow the cell cycle on flow cytometry. The population discrimination algorithm Watson pragmatic model was used to divide the cycle data into G0/G1, S and M/G2 phases according to the dye fluorescence intensity signal as described elsewhere [38,39]. **a)** BV173 cell cycle of control cells (grey). Flow cytometry histogram with separation by Watson pragmatic model into G0/G1, S and M/G2. Cells were cultured on supplemented medium without antibiotic. **b)** Analysis of the influence of pepR and pepM in BV173 cell cycle G0/G1, S and M/G2 phases by flow cytometry. The cell population (100%) is under a division stage (percentage), which is carefully assigned by Watson pragmatic model. Cells were incubated with 0.5 or 5 μM of pepM (green and blue, respectively) and 0.5 or 5 μM of pepR (red and orange, respectively) and the cell cycle analyzed. The percentage of the cells (average ± SD) in each cell cycle phase is represented ($n > 15$). **c)** Representative cell cycle histogram of the average population for each condition tested (0.5 μM pepM – green, 5 μM pepM – blue, 0.5 μM pepR – red, 5 μM pepR – orange). Cell cycle percentages were analyzed by a two-tailed *t*-test (**** - $p < 0.0001$; *** - $p = 0.0002$; ** - $p = 0.008$; * - $p = 0.03$).

effective action against BV173 cells: the siRNA targets directly the major hallmark of the pathology, the *Bcr-Abl1* fusion gene, while the vector co-operatively reduces BV173 leukaemogenic proliferation.

It is curious how, while not acting as a successful siRNA delivery agent to fight CML, pepR shows an appealing anticancer activity against CML. As for pepM, the dichotomy of having both efficient siRNA delivery together with anticancer activity (with no inducing of significant cellular stress) is even more promising for further biotechnological refinement. These results can open the way to explore other CPP formulations such as HIV-1 Tat peptide, or the synthetic Arginine-based CPP to deliver siRNA and act as anticancer molecules. The explanation of their anticancer activity is multifactorial, and their mechanism of action is still in debate [61]. ACP can have intracellular targets, requiring thus CPP properties, and interfere with cellular pathways (as the ones described in this work) or act at the membrane level. Notwithstanding, both rely on the fact that it is dependent on lipid membrane interactions, and the cell membrane of cancer molecules is altered in its lipid composition in what respects to normal healthy cells. Changes in cellular content of external phosphatidilserine and or cholesterol content may suffice to increase peptide-lipid interactions, and induce more severe peptide-induced lipid alterations (such as formation of pores, micelles, etc.) [61]. Several of the current anticancer peptides described [62] may have had their origin as previous CPP or antimicrobial peptides (AMP). It is their narrow inter-correlation of biological activities and weighting of several molecular descriptors that promote such interesting findings of a CPP becoming an ACP (anticancer molecule) or a AMP having ACP activity. This was what was observed in this manuscript, two already described CPP [26,27] were found to be ACP against

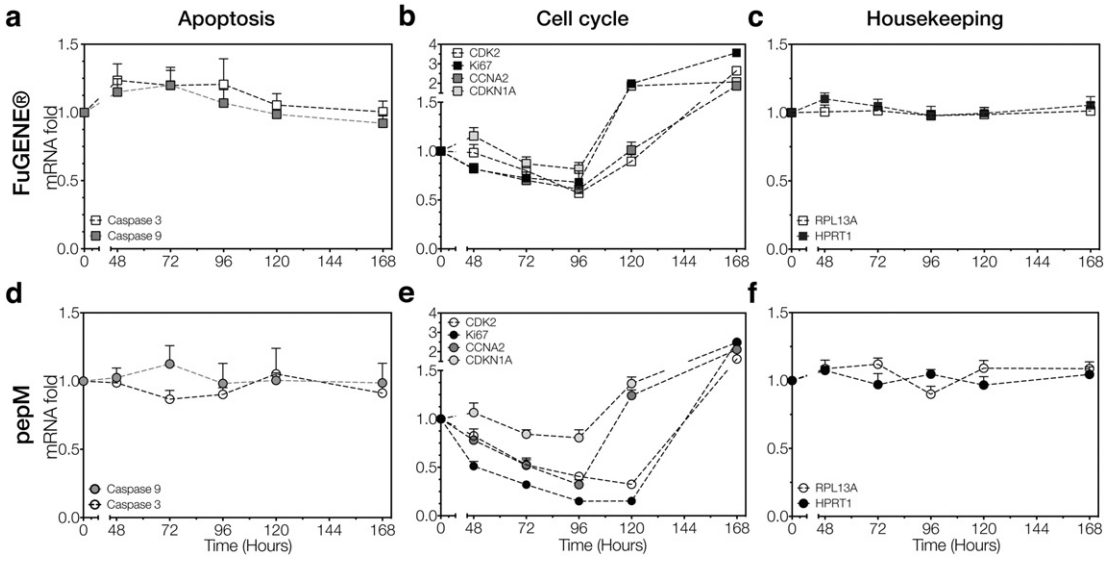

Fig. 6. pepM and FuGENE influence on BV173 gene expression. BV173 qRT-PCR of mRNA expression levels of housekeeping/cell stress RPL13A (white) and HPRT1 (black) genes (**c** and **f**), cell proliferation ki67 (black), cell cycle CDK2 (white), CCDN2 (dark grey) and CDKN1A (light grey) genes (**b** and **e**) and, cell apoptosis Caspase 3 (white) and Caspase 9 (grey) genes after the addition of either pepM (circles) or FuGENE (square). Relative expression values were analyzed by the two-tailed *t*-test. mRNA expression levels were analyzed by real-time PCR 48 h, 72 h, 96 h, 120 h and 168 h after the addition of the transfection agent. In every case, the resulting data are the mean of three experiments with standard deviation.

CML. Being R8, HIV-1 Tat and penetratin already described as CPP and in some occasions as AMP [63], it would not be surprising that these vectors would act effectively as bioportides such as in this work pepM, delivering an siRNA molecule and interfere with cell cycle. Though, according to Kuo et al. [43] the influence of R8 in cell immune response is thus more significant than what observed for pepM. To conclude, these formulations may present some degree of cellular specificity, however, since the target is a circulating blood cell, the molecule would rapidly diffuse among such cells, obviating concentrating in other tissues or organs in a long-term exposure. Even though, the refinement of these peptide-based formulations could be envisioned with the conjugation of PEG moieties and tumor homing sequences targeting CML in order to overcome issues regarding non-specific interactions with circulating negatively charged molecules, serum albumin aggregation and cellular specificity.

4. Conclusions

The present work reveals the potential of CPP-siRNA conjugates to tackle genetic disorders. Specifically we aimed at targeting the *Bcr-Abl1* gene mutation responsible for CML. Five novel siRNA molecules conjugated with two novel DENV C-derived CPPs, pepR and pepM, were tested. The conjugate of siRNA-CF-3 with pepM was found to be the optimal formulation causing maximal *Bcr-Abl1* mRNA inhibition for a longer time (120 h). Most importantly, a thorough analysis of the genome-wide influence of peptide vectors on cell homeostasis and expression profiles has been performed, which in combination with Kuo and co-workers data [43], elucidates the implications on cellular homeostasis about using peptide-based formulations. Our analysis shows that these CPPs do not significantly affect key cellular pathways or trigger apoptotic events at the concentration required for siRNA delivery but that the vectors by themselves intervene in a (co-adjuvant) therapeutic manner by perturbing the cellular pathways triggered by *Bcr-Abl1* signaling.

Another significant finding is that CPPs have a direct influence on cytoskeleton protein expression levels. CPPs were known to interact with cytoskeleton proteins such as actin [56], but never heretofore shown to influence cytoskeleton expression levels.

In conclusion, pepM has proven its efficacy as and non-toxic siRNA delivery agent in the era of genetic therapy, and shown how CPP-based delivery systems can be applied in cancer therapies. Moreover, both pepM and pepR have depicted interesting anticancer properties that merit further explorations.

Associated content

Additional supporting information may be found online. Prediction, design and selection of anti-*Bcr-Abl1* siRNA using Ambion® on-line server. Sequences and genome ID are at GENES_ID.xls file. Table S1 and S2 resume the target sequences and 5 siRNA chosen for *in vitro* testing. *Section 2:* Example of the usage of Fiji's analysis software plugin Cell counter for quantitative microscopy analysis of expression of BV173 GFP expression levels and transfection efficacy – Figure S1. *Section 3:* Chromosomal location of the genes up- and down-regulated after incubation with pepR and pepM. Scatter plot of expression levels of pepR and pepM vs. control BV173 cells that indicate the threshold levels to identify up- and down-regulated genes. Genes with 2-fold variation (up or down) were selected. *Supplementary Table S4.xls:* List of identified targets for pepR and pepM microarray. Fold change vs. untreated BV173 cells is showed with *p*-value of the change significance. Cellular function described for each gene target as well as the cellular pathways involved is also described. *Section 4*: Table S3 with the primer sequences used in qPCR for *BCR-ABL, GAPDH, CASP3, CASP9, CDK2, KI67, CCNA2, CDKN1A, RPL13A, HPRT1* genes.

Competing financial interests statements

The authors have no competing financial interests.

Acknowledgements

This work was supported by Fundação para a Ciência e Tecnologia – Ministério da Educação e Ciência (FCT-MEC, Portugal) [PTDC/QUI-BIQ/112929/2009], by Gabinete de Apoio à Investigação Científica, Tecnológica e Inovação (GAPIC – grants n° 20110007 and 20120006), Fundação AstraZeneca Innovative Competition 2013 (iMed 5.0), the European Union [FP7-HEALTH-F3-2008-223414 (LEISHDRUG)], by the Spanish Ministry of Economy and Competitiveness (SAF2011-24899) and the Generalitat de Catalunya (2009 SGR 492). JMF acknowledges FCT-MEC for PhD fellowship SFRH/BD/70423/2010 and ASV for fellowship IF/00803/2012 under the FCT Investigator Programme.

Appendix A. Supplementary data

Supplementary data to this article can be found online at http://dx.doi.org/10.1016/j.jconrel.2016.11.027.

References

[1] E. De Braekeleer, N. Douet-Guilbert, D. Rowe, N. Bown, F. Morel, C. Berthou, et al., ABL1 fusion genes in hematological malignancies: a review, Eur. J. Haematol. 86 (2011) 361–371, http://dx.doi.org/10.1111/j.1600-0609.2011.01586.x.
[2] R. Hehlmann, A. Hochhaus, M. Baccarani, European LeukemiaNet, chronic myeloid leukaemia, Lancet 370 (2007) 342–350, http://dx.doi.org/10.1016/S0140-6736(07)61165-9.
[3] G.K. Lambert, A.-K. Duhme-Klair, T. Morgan, M.K. Ramjee, The background, discovery and clinical development of BCR-ABL inhibitors, Drug Discov. Today 18 (2013) 992–1000, http://dx.doi.org/10.1016/j.drudis.2013.06.001.
[4] B.J. Druker, Translation of the Philadelphia chromosome into therapy for CML, Blood 112 (2008) 4808–4817, http://dx.doi.org/10.1182/blood-2008-07-077958.
[5] M. Breccia, G. Alimena, Occurrence and current management of side effects in chronic myeloid leukemia patients treated frontline with tyrosine kinase inhibitors, Leuk. Res. 37 (2013) 713–720, http://dx.doi.org/10.1016/j.leukres.2013.01.021.
[6] J.M. Goldman, Chronic myeloid leukemia: current treatment options, Blood 98 (2001) 2039–2042, http://dx.doi.org/10.1182/blood.V98.7.2039.
[7] B.S.M. MHS, B.D.S. MD, Treatment options for patients with chronic myeloid leukemia who are resistant to or unable to tolerate imatinib, Clin. Ther. 32 (2010) 804–820, http://dx.doi.org/10.1016/j.clinthera.2010.05.003.
[8] Y. Zhao, L. Zhao, L. Zhou, Y. Zhi, J. Xu, Z. Wei, et al., Quantum dot conjugates for targeted silencing of bcr/abl gene by RNA interference in human myelogenous leukemia K562 cells, J. Nanosci. Nanotechnol. 10 (2010) 5137–5143http://eutils.ncbi.nlm.nih.gov/entrez/eutils/elink.fcgi?dbfrom=pubmed&id=21125862&retmode=ref&cmd=prlinks.
[9] Y. Arthanari, A. Pluen, R. Rajendran, H. Aojula, C. Demonacos, Delivery of therapeutic shRNA and siRNA by Tat fusion peptide targeting bcr–abl fusion gene in Chronic Myeloid Leukemia cells, J. Control. Release 145 (2010) 272–280, http://dx.doi.org/10.1016/j.jconrel.2010.04.011.
[10] J. Valencia-Serna, H. Gul-Uludağ, P. Mahdipoor, X. Jiang, H. Uludağ, Investigating siRNA delivery to chronic myeloid leukemia K562 cells with lipophilic polymers for therapeutic BCR-ABL down-regulation, J. Control. Release 172 (2013) 495–503, http://dx.doi.org/10.1016/j.jconrel.2013.05.014.
[11] I.R. de Figueiredo, J.M. Freire, L. Flores, A.S. Veiga, M.A.R.B. Castanho, Cell-penetrating peptides: a tool for effective delivery in gene-targeted therapies, IUBMB Life. 66 (2014) 182–194, http://dx.doi.org/10.1002/iub.1257.
[12] A. Bolhassani, Potential efficacy of cell-penetrating peptides for nucleic acid and drug delivery in cancer, Biochim. Biophys. Acta 1816 (2011) 232–246, http://dx.doi.org/10.1016/j.bbcan.2011.07.006.
[13] D.M. Copolovici, K. Langel, E. Eriste, Ü. Langel, Cell-penetrating peptides: design, synthesis, and applications, ACS Nano 8 (2014) 1972–1994, http://dx.doi.org/10.1021/nn4057269.
[14] N. Svensen, J.G.A. Walton, M. Bradley, Peptides for cell-selective drug delivery, Trends Pharmacol. Sci. 33 (2012) 186–192, http://dx.doi.org/10.1016/j.tips.2012.02.002.
[15] B.P. Timko, K. Whitehead, W. Gao, D.S. Kohane, O. Farokhzad, D. Anderson, et al., Advances in drug delivery, Annu. Rev. Mater. Res. 41 (2011) 1–20, http://dx.doi.org/10.1146/annurev-matsci-062910-100359.
[16] P. Jarver, I. Mäger, Ü. Langel, In vivo biodistribution and efficacy of peptide mediated delivery, Trends Pharmacol. Sci. 31 (2010) 528–535, http://dx.doi.org/10.1016/j.tips.2010.07.006.
[17] F. Milletti, Cell-penetrating peptides: classes, origin, and current landscape, Drug Discov. Today 17 (2012) 850–860, http://dx.doi.org/10.1016/j.drudis.2012.03.002.
[18] F. Heitz, M.C. Morris, G. Divita, Twenty years of cell-penetrating peptides: from molecular mechanisms to therapeutics, Brit. J. Pharmacol. 157 (2009) 195–206, http://dx.doi.org/10.1111/j.1476-5381.2009.00057.x.

[19] A. Gautam, H. Singh, A. Tyagi, K. Chaudhary, R. Kumar, P. Kapoor, et al., CPPsite: a curated database of cell penetrating peptides, Database 2012 (bas015) (2012), http://dx.doi.org/10.1093/database/bas015.
[20] T. Lehto, K. Kurrikoff, Ü. Langel, Cell-penetrating peptides for the delivery of nucleic acids, Expert Opin. Drug Deliv. 9 (2012) 823–836, http://dx.doi.org/10.1517/17425247.2012.689285.
[21] I. Nakase, H. Akita, K. Kogure, A. Gräslund, Ü. Langel, H. Harashima, et al., Efficient intracellular delivery of nucleic acid pharmaceuticals using cell-penetrating peptides, Acc. Chem. Res. 45 (2012) 1132–1139, http://dx.doi.org/10.1021/ar200256e.
[22] J. Nguyen, F.C. Szoka, Nucleic acid delivery: the missing pieces of the puzzle? Acc. Chem. Res. 45 (2012) 1153–1162, http://dx.doi.org/10.1021/ar3000162.
[23] I. Nakase, G. Tanaka, S. Futaki, Cell-penetrating peptides (CPPs) as a vector for the delivery of siRNAs into cells, Mol. BioSyst. 9 (2013) 855–861, http://dx.doi.org/10.1039/c2mb25467k.
[24] J. Howl, S. Matou-Nasri, D.C. West, M. Farquhar, J. Slaninová, C.-G. Östenson, et al., Bioportide: an emergent concept of bioactive cell-penetrating peptides, Cell. Mol. Life Sci. 69 (2012) 2951–2966, http://dx.doi.org/10.1007/s00018-012-0979-4.
[25] M. Lukanowska, J. Howl, S. Jones, Bioportides: bioactive cell-penetrating peptides that modulate cellular dynamics, Biotechnol. J. 8 (2013) 918–930, http://dx.doi.org/10.1002/biot.201200335.
[26] J.M. Freire, A.S. Veiga, T.M. Conceição, W. Kowalczyk, R. Mohana-Borges, D. Andreu, et al., Intracellular nucleic acid delivery by the supercharged dengue virus capsid protein, PLoS One 8 (2013), e81450, http://dx.doi.org/10.1371/journal.pone.0081450.s001.
[27] J.M. Freire, A.S. Veiga, I. Rego de Figueiredo, B.G. de la Torre, N.C. Santos, D. Andreu, et al., Nucleic acid delivery by cell penetrating peptides derived from dengue virus capsid protein: design and mechanism of action, FEBS J. 281 (2014) 191–215, http://dx.doi.org/10.1111/febs.12587.
[28] A.S.M. Kumar, G.E.C.V. Reddy, Y. Rajmane, S. Nair, S. Pai Kamath, G. Sreejesh, et al., siRNAs encapsulated in recombinant capsid protein derived from Dengue serotype 2 virus inhibits the four serotypes of the virus and proliferation of cancer cells, J. Biotechnol. 193C (2014) 23–33, http://dx.doi.org/10.1016/j.jbiotec.2014.11.003.
[29] L. Pegoraro, L. Matera, J. Ritz, A. Levis, A. Palumbo, G. Biagini, Establishment of a Ph1-positive human cell line (BV173), J. Natl. Cancer Inst. 70 (1983) 447–453.
[30] M. Koldehoff, L. Kordelas, D.W. Beelen, A.H. Elmaagacli, Small interfering RNA against BCR-ABL transcripts sensitize mutated T315I cells to nilotinib, Haematologica 95 (2010) 388–397, http://dx.doi.org/10.3324/haematol.2009.016063.
[31] G.B. Fields, R.L. Noble, Solid phase peptide synthesis utilizing 9-fluorenylmethoxycarbonyl amino acids, Int. J. Pept. Protein Res. 35 (1990) 161–214.
[32] C.S. Alves, M.N. Melo, H.G. Franquelim, R. Ferre, M. Planas, L. Feliu, et al., *Escherichia coli* Cell surface perturbation and disruption induced by antimicrobial peptides BP100 and pepR, J. Biol. Chem. 285 (2010) 27536–27544, http://dx.doi.org/10.1074/jbc.M110.130955.
[33] J.M. Freire, A.S. Veiga, B.G. de la Torre, D. Andreu, M.A.R.B. Castanho, Quantifying molecular partition of cell-penetrating peptide-cargo supramolecular complexes into lipid membranes: optimizing peptide-based drug delivery systems, J. Pept. Sci. 19 (2013) 182–189, http://dx.doi.org/10.1002/psc.2477.
[34] J.M. Freire, A.S. Veiga, B.G. de la Torre, N.C. Santos, D. Andreu, A.T. Da Poian, et al., Peptides as models for the structure and function of viral capsid proteins: insights on dengue virus capsid, Biopolymers 100 (2013) 325–336, http://dx.doi.org/10.1002/bip.22266.
[35] A. Roy, A. Kucukural, Y. Zhang, I-TASSER: a unified platform for automated protein structure and function prediction, Nat. Protoc. 5 (2010) 725–738, http://dx.doi.org/10.1038/nprot.2010.5.
[36] W. DeLano, The PyMOL Molecular Graphics System (DeLano Scientific LLC, Palo Alto, CA), Wiley-Interscience, 2008http://scholar.google.com/scholar?q=related:DLqWH9so7N4J:scholar.google.com/&hl=en&num=30&as_sdt=0,5.
[37] J. Schindelin, I. Arganda-Carreras, E. Frise, V. Kaynig, M. Longair, T. Pietzsch, et al., Fiji: an open-source platform for biological-image analysis, Nat. Methods 9 (2012) 676–682, http://dx.doi.org/10.1038/nmeth.2019.
[38] J. Van Dongen, E.A. Macintyre, J.A. Gabert, E. Delabesse, V. Rossi, G. Saglio, et al., Standardized RT-PCR analysis of fusion gene transcripts from chromosome aberrations in acute leukemia for detection of minimal residual disease, Leukemia 13 (1999) 1901–1928.
[39] F. Belloc, P. Dumain, M.R. Boisseau, C. Jalloustre, J. Reiffers, P. Bernard, et al., A flow cytometric method using Hoechst 33342 and propidium iodide for simultaneous cell cycle analysis and apoptosis determination in unfixed cells, Cytometry 17 (1994) 59–65, http://dx.doi.org/10.1002/cyto.990170108.
[40] P. Pozarowski, Z. Darzynkiewicz, Analysis of cell cycle by flow cytometry, Methods Mol. Biol. 281 (2004) 301–311, http://dx.doi.org/10.1385/1-59259-811-0:301.
[41] J.V. Watson, S.H. Chambers, P.J. Smith, A pragmatic approach to the analysis of DNA histograms with a definable G1 peak, Cytometry 8 (1987) 1–8, http://dx.doi.org/10.1002/cyto.990080101.
[42] D.W. Bartlett, Insights into the kinetics of siRNA-mediated gene silencing from live-cell and live-animal bioluminescent imaging, Nucleic Acids Res. 34 (2006) 322–333, http://dx.doi.org/10.1093/nar/gkj439.
[43] J.-H.S. Kuo, M.-S. Jan, Y.-L. Lin, C. Lin, Interactions between octaarginine and U-937 human macrophages: global gene expression profiling, superoxide anion content, and cytokine production, J. Control. Release 139 (2009) 197–204, http://dx.doi.org/10.1016/j.jconrel.2009.07.006.
[44] M.B. Eisen, P.T. Spellman, P.O. Brown, D. Botstein, Cluster analysis and display of genome-wide expression patterns, Proc. Natl. Acad. Sci. 95 (1998) 14863–14868.
[45] R.W. Carthew, E.J. Sontheimer, Origins and mechanisms of miRNAs and siRNAs, Cell 136 (2009) 642–655, http://dx.doi.org/10.1016/j.cell.2009.01.035.
[46] M. Chekulaeva, W. Filipowicz, Mechanisms of miRNA-mediated post-transcriptional regulation in animal cells, Curr. Opin. Cell Biol. 21 (2009) 452–460, http://dx.doi.org/10.1016/j.ceb.2009.04.009.
[47] M. Selbach, B. Schwanhäusser, N. Thierfelder, Z. Fang, R. Khanin, N. Rajewsky, Widespread changes in protein synthesis induced by microRNAs, Nature 455 (2008) 58–63, http://dx.doi.org/10.1038/nature07228.
[48] R.S. Pillai, S.N. Bhattacharyya, W. Filipowicz, Repression of protein synthesis by miRNAs: how many mechanisms? Trends Cell Biol. 17 (2007) 118–126, http://dx.doi.org/10.1016/j.tcb.2006.12.007.
[49] A. Kozomara, S. Griffiths-Jones, miRBase: annotating high confidence microRNAs using deep sequencing data, Nucleic Acids Res. 42 (2014) D68–D73, http://dx.doi.org/10.1093/nar/gkt1181.
[50] H. Hamzeiy, J. Allmer, M. Yousef, Computational methods for microRNA target prediction, Methods Mol. Biol. 1107 (2014) 207–221, http://dx.doi.org/10.1007/978-1-62703-748-8_12.
[51] M.S. Ebert, P.A. Sharp, Roles for MicroRNAs in conferring robustness to biological processes, Cell 149 (2012) 515–524, http://dx.doi.org/10.1016/j.cell.2012.04.005.
[52] D.M. Garcia, D. Baek, C. Shin, G.W. Bell, A. Grimson, D.P. Bartel, Weak seed-pairing stability and high target-site abundance decrease the proficiency of lsy-6 and other microRNAs, Nat. Struct. Mol. Biol. 18 (2011) 1139–1146, http://dx.doi.org/10.1038/nsmb.2115.
[53] E.K. Greuber, P. Smith-Pearson, J. Wang, A.M. Pendergast, Role of ABL family kinases in cancer: from leukaemia to solid tumours, Nat. Rev. Cancer 13 (2013) 559–571, http://dx.doi.org/10.1038/nrc3563.
[54] A.-X. Wang, X.-Y. Qi, Targeting RAS/RAF/MEK/ERK signaling in metastatic melanoma, IUBMB Life 65 (2013) 748–758, http://dx.doi.org/10.1002/iub.1193.
[55] D. Ribeiro, A. Melão, J.T. Barata, IL-7R-mediated signaling in T-cell acute lymphoblastic leukemia, Adv Biol Regul. 53 (2013) 211–222, http://dx.doi.org/10.1016/j.jbior.2012.10.005.
[56] A. Mishra, G.H. Lai, N.W. Schmidt, V.Z. Sun, A.R. Rodriguez, R. Tong, et al., Translocation of HIV TAT peptide and analogues induced by multiplexed membrane and cytoskeletal interactions, Proc. Natl. Acad. Sci. U. S. A. 108 (2011) 16883–16888, http://dx.doi.org/10.1073/pnas.1108795108.
[57] G.M. Cragg, D.J. Newman, Natural products: a continuing source of novel drug leads, Biochim. Biophys. Acta 1830 (2013) 3670–3695, http://dx.doi.org/10.1016/j.bbagen.2013.02.008.
[58] C.E. Symonds, U. Galderisi, A. Giordano, Aging of the inceptive cellular population: the relationship between stem cells and aging, Aging (Albany NY) 1 (2009) 372–381.
[59] G. Davidson, C. Niehrs, Emerging links between CDK cell cycle regulators and Wnt signaling, Trends Cell Biol. 20 (2010) 453–460, http://dx.doi.org/10.1016/j.tcb.2010.05.002.
[60] J. Gerdes, H. Lemke, H. Baisch, H.H. Wacker, U. Schwab, H. Stein, Cell cycle analysis of a cell proliferation-associated human nuclear antigen defined by the monoclonal antibody Ki-67, J. Immunol. 133 (1984) 1710–1715.
[61] D. Gaspar, A.S. Veiga, M.A.R.B. Castanho, From antimicrobial to anticancer peptides. A review, Front. Microbiol. 4 (2013) 294, http://dx.doi.org/10.3389/fmicb.2013.00294.
[62] A. Tyagi, A. Tuknait, P. Anand, S. Gupta, M. Sharma, D. Mathur, et al., CancerPPD: a database of anticancer peptides and proteins, Nucleic Acids Res. 43 (2015) D837–D843, http://dx.doi.org/10.1093/nar/gku892.
[63] K. Split, I. Neundorf, Antimicrobial peptides with cell-penetrating peptide properties and vice versa, Eur. Biophys. J. 40 (2011) 387–397, http://dx.doi.org/10.1007/s00249-011-0682-7.
[64] H. Ohba, et al., Inhibition of bcr-abl and/orc-abl gene expression by small interfering, double-stranded RNAs, Cancer 101 (2004) 1390–1403.
[65] X. Huang, et al., Gene expression profiles in BCL11B-siRNA treated malignant T cells, J. Hematol. Oncol. 4 (2011) 23.